THE JOURNAL OF PHYSICAL CHEMISTRY Letters

Letter

Cite This: J. Phys. Chem. Lett. 2019, 10, 4668−4674

pubs.acs.org/JPCL

Capturing the Dynamic Correlation for Arbitrary Spin-Symmetry CASSCF Reference with Adiabatic Connection Approaches: Insights into the Electronic Structure of the Tetramethyleneethane Diradical

Ewa Pastorczak,*,† Michał Hapka,*,‡ Libor Veis,¶ and Katarzyna Pernal*,†

†Institute of Physics, Lodz University of Technology, ul. Wolczanska 219, 90-924 Lodz, Poland

‡Faculty of Chemistry, University of Warsaw, ul. L. Pasteura 1, 02-093 Warsaw, Poland

¶J. Heyrovský Institute of Physical Chemistry, Academy of Sciences of the Czech Republic, v.v.i., Dolejškova 3, 18223 Prague 8, Czech Republic

Supporting Information

ABSTRACT: The recently proposed approach to multireference dynamic correlation energy based on the adiabatic connection (AC) is extended to an arbitrary spin symmetry of the reference state. We show that both the spin-free AC approach and its computationally inexpensive approximation, AC0, when combined with a complete active space wave function, constitute viable alternatives to the perturbation-based and density-functional-based multiconfiguration methods. In particular, the AC0 approach, thanks to its favorable scaling with the system size and the size of the active space, allows for treating larger systems than its perturbation-based counterparts while maintaining comparable accuracy. We show the method's robustness on illustrative chemical systems, including the elusive tetramethyleneethane (TME) diradical, potential energy surfaces of which present a challenge to most computational approaches. For the latter system, AC0 outperforms other methods, staying in close agreement with the full configuration interaction quantum Monte Carlo benchmark. A careful analysis of the contributions to the correlation energy of TME's lowest singlet and triplet states reveals the subtle interplay of the dynamic and static correlation as the key to understanding the shape of the diradical's potential energy surfaces.

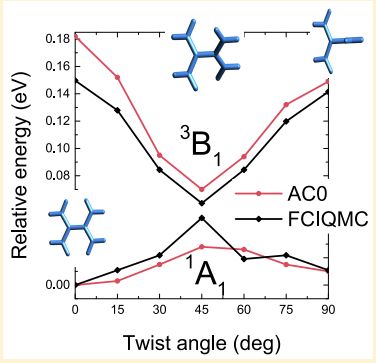

Simultaneous description of different spin-symmetry states of a molecule is a challenging task, especially if either of the states is of a multireference character. To obtain, for example, the correct value of the singlet−triplet (S−T) gap of such a system, the employed computational method has to be able to describe both the singlet and the triplet states with the same accuracy, usually at the level of sub-eV. The underlying difficulty amounts primarily to simultaneous description of both static and dynamic correlation effects. One way to tackle this problem is by combining a sufficiently flexible multiconfiguration wave function, usually of the complete active space (CAS) ansatz, with a dynamic-correlation correction. Most popular approaches (notwithstanding the successes of methods like Quantum Monte Carlo (QMC)[1] or multiconfiguration density functional theory[2,3]), such as the Complete Active Space Perturbation Theory (CASPT2)[4,5] and *n*-Electron Valence State Perturbation Theory (NEVPT2)[6,7] use a perturbation-based correction to account for the dynamic correlation. Even for small systems, like the methylene molecule, the accuracy of perturbation-based approaches may prove insufficient for reliable S−T gap predictions.[8−10] The problem becomes particularly aggravated for large systems with small S−T gaps because both the accuracy and cost of perturbation correction computations depend heavily on the quality of the used wave function. Hence arises the need for new, computationally efficient ways of including the description of dynamic correlation into multireference approaches.

Recently, by adopting the adiabatic connection (AC) formalism, we have derived an expression for the correlation energy for a broad class of multireference wave functions.[11−13] The latter has been assumed to be a generalized group-product function,[14] the CAS function being a special case of such an ansatz.[12] The AC correlation energy expression in the chosen spin-orbital basis set reads

$$E_{\mathrm{corr}}^{\mathrm{AC}} = \int_0^1 W^{\lambda}\,\mathrm{d}\lambda \tag{1}$$

$$W^{\lambda} = \frac{1}{2}\sum_{pqrs}{}' \left(\sum_{\nu\neq 0}\gamma_{pr}^{\lambda,\nu}\gamma_{qs}^{\lambda,\nu} + (\gamma_{ps}-\delta_{ps})\gamma_{rq}\right)\langle rs|pq\rangle \tag{2}$$

The expression has been obtained for a particular choice of the AC Hamiltonian $\hat{H}^{\lambda}$ (for its definition, cf. refs 11 and 12), and λ is a coupling parameter connecting a group-uncorrelated limit ($\lambda = 0$) with the full-correlation limit ($\lambda = 1$). $\langle rs|pq\rangle$ stands for a two-electron integral in the usual $x_1x_2x_1x_2$ convention. Elements

Received: June 2, 2019
Accepted: July 29, 2019
Published: July 29, 2019

DOI: 10.1021/acs.jpclett.9b01582
J. Phys. Chem. Lett. 2019, 10, 4668−4674

$\{\gamma^{\lambda,\nu}_{pq}\}$ in eq 2 are one-electron transition reduced density matrix elements defined as $\gamma^{\lambda,\nu}_{pq} = \langle\Psi^{\lambda}|\hat{a}^{\dagger}_{q}\hat{a}_{p}|\Psi^{\lambda}_{\nu}\rangle$, where Ψ^{λ} and Ψ^{λ}_{ν} are eigenstates of the AC Hamiltonian, $\hat{H}^{\lambda}\Psi^{\lambda}_{\nu} = E^{\lambda}_{\nu}\Psi^{\lambda}_{\nu}$. In particular, Ψ^{λ} is an eigenstate connecting smoothly with Ψ^{ref} at $\lambda = 0$, Ψ^{ref} being a reference wave function, e.g., a CAS function describing a state of interest.[13] The one-electron reduced density matrix (1-RDM) corresponds to a reference function, $\gamma_{pq} = \langle\Psi^{\mathrm{ref}}|\hat{a}^{\dagger}_{q}\hat{a}_{p}|\Psi^{\mathrm{ref}}\rangle$. The prime sign in eq 2 indicates that the indices of the spin-orbitals p, q, r, s cannot simultaneously belong to the same group of orthogonal spin-orbitals.

Until now, the AC correction has been developed and applied for reference wave functions in singlet spin symmetry. Here, we extend the AC and its approximation, AC0, to an arbitrary spin symmetry of the reference state. After carrying out summation in eq 2 with respect to spin coordinates, one is led to

$$W^{\lambda} = \frac{1}{2}\sum_{pqrs}{}' \left[\sum_{\nu\neq 0}(\gamma^{\lambda,\nu}_{p_\alpha r_\alpha} + \gamma^{\lambda,\nu}_{p_\beta r_\beta})(\gamma^{\lambda,\nu}_{q_\alpha s_\alpha} + \gamma^{\lambda,\nu}_{q_\beta s_\beta}) + (\gamma_{p_\alpha s_\alpha}\gamma_{r_\alpha q_\alpha} + \gamma_{p_\beta s_\beta}\gamma_{r_\beta q_\beta}) - \delta_{ps}(\gamma_{r_\alpha q_\alpha} + \gamma_{r_\beta q_\beta})\right]\langle rs|pq\rangle \tag{3}$$

where p_α and p_β are the spin-up and spin-down components of the spin-orbital p. At first sight, it seems that for nonsinglet states one needs to know separately the $\alpha\alpha$ and $\beta\beta$ spin-blocks (and not only their sum $\alpha\alpha + \beta\beta$) of the 1-RDM. Notice, however, that for the CAS function (or, in general, an MCSCF ansatz) there are only inactive (doubly occupied), active, and virtual (unoccupied) orbital subsets and only for the active−active block $\gamma^{\alpha\alpha} \neq \gamma^{\beta\beta}$ for a nonsinglet state. Exploiting that γ_{pq} elements are different from zero only if p, q both correspond to either active or inactive spin-orbitals, it is straightforward to see that the integrand W^{λ} depends only on the spin-summed density matrices, and in the representation of the reference natural orbitals, it reads

$$W^{\lambda} = \frac{1}{2}\sum_{pqrs}{}' \left[\sum_{\nu\neq 0}\overline{\gamma}^{\lambda,\nu}_{pr}\overline{\gamma}^{\lambda,\nu}_{qs} + 2\delta_{ps}\delta_{rq}(n_p - 1)n_q\right]\langle rs|pq\rangle \tag{4}$$

where

$$\gamma_{pq} = \gamma_{p_\alpha q_\alpha} + \gamma_{p_\beta q_\beta} = 2n_p\delta_{pq} \tag{5}$$

and

$$\overline{\gamma}^{\lambda,\nu}_{pr} = \gamma^{\lambda,\nu}_{p_\alpha r_\alpha} + \gamma^{\lambda,\nu}_{p_\beta r_\beta} \tag{6}$$

(α and β indicate spin parts).

We have proposed to employ Rowe's equation of motion theory[15] in the extended random phase approximation (ERPA)[16,17] to obtain transition density matrices. Within Rowe's theory, a state $|\Psi_\nu\rangle$ is generated from an arbitrary state $|\Psi\rangle$ upon action of an excitation operator $\hat{O}^{\dagger}_{\nu}$, which in the ERPA approximation is truncated to include only single excitations

$$\hat{O}^{\dagger}_{\nu} = \sum_{p>q}[\mathbf{X}_\nu]_{pq}\hat{a}^{\dagger}_{p}\hat{a}_{q} + \sum_{p>q}[\mathbf{Y}_\nu]_{pq}\hat{a}^{\dagger}_{q}\hat{a}_{p} \tag{7}$$

The operator $\hat{O}^{\dagger}_{\nu}$ written as in eq 7 is, in general, not spin-adapted. A discussion of spin adaptation provided, e.g., in ref 18 shows that imposing a restriction on $\alpha\alpha$ and $\beta\beta$ elements of the coefficients X and Y as follows

$$[\mathbf{X}_\nu]_{p_\alpha q_\alpha} = [\mathbf{X}_\nu]_{p_\beta q_\beta} \tag{8}$$

$$[\mathbf{Y}_\nu]_{p_\alpha q_\alpha} = [\mathbf{Y}_\nu]_{p_\beta q_\beta} \tag{9}$$

results in preservation of the spin symmetry when operating with $\hat{O}^{\dagger}_{\nu}$ on $|\Psi\rangle$, namely, if the total spin of $|\Psi\rangle$ is S, then so is the spin of the state $|\Psi_\nu\rangle$. Notice that the spin-preserving adaptation of the excitation operator is not the only possible choice. In general, states of different spin symmetry than S can be coupled by the ERPA equations and may have a nonzero contribution to the correlation energy in eq 4. Accounting for them would greatly complicate and increase the computational cost of the AC approach, and we limit the space of excitation operators in the ERPA approximation to the spin-preserving ones defined by eqs 8 and 9. Employing ERPA approximation to the transition density matrices following from Rowe's equation[15,19]

$$\gamma^{0\nu}_{pq} = \sum_{t<p}[\mathbf{X}_\nu]_{pt}\gamma_{tq} - \sum_{t>q}[\mathbf{X}_\nu]_{tq}\gamma_{pt} + \sum_{t>p}[\mathbf{Y}_\nu]_{tp}\gamma_{tq} - \sum_{t<q}[\mathbf{Y}_\nu]_{qt}\gamma_{pt} \tag{10}$$

together with eqs 8 and 9 allows one to write the integrand in eq 4 as a spin-free formula (the indices pertain to orbitals) reading

$$W^{\lambda} = 2\sum_{\substack{p>q\\ r>s}}{}' \left\{(n_p - n_q)(n_r - n_s)\sum_{\nu}([\mathbf{Y}^{\lambda}_{\nu}]_{pq} - [\mathbf{X}^{\lambda}_{\nu}]_{pq})([\mathbf{Y}^{\lambda}_{\nu}]_{rs} - [\mathbf{X}^{\lambda}_{\nu}]_{rs}) - \frac{1}{2}[n_p(1 - n_q) + n_q(1 - n_p)]\delta_{pr}\delta_{qs}\right\}\langle pr|qs\rangle \tag{11}$$

The ERPA vectors $[\mathbf{X}^{\lambda}_{\nu}, \mathbf{Y}^{\lambda}_{\nu}]$ follow from the spin-adapted ERPA equations with spin-free matrices $\mathcal{A}^{\lambda}$ and $\mathcal{B}^{\lambda}$ defined as $[\mathcal{A}^{\lambda}]_{pqrs} = [\mathcal{B}^{\lambda}]_{pqsr} = \sum_{\sigma,\sigma'}\langle\Psi^{\mathrm{ref}}|[\hat{a}^{\dagger}_{p_\sigma}\hat{a}_{q_\sigma}, [\hat{H}^{\lambda}, \hat{a}^{\dagger}_{s_{\sigma'}}\hat{a}_{r_{\sigma'}}]]|\Psi^{\mathrm{ref}}\rangle$. They are given solely in terms of the spin-summed 1-and 2-RDMs (for their explicit form, see the Supporting Information (SI)).

In refs 12 and 13, we have shown that the cost of computing the AC correlation energy can be greatly reduced, without a loss in accuracy, by employing the AC0 approximation. The AC0 results from linear expansion of the AC integrand, W^{λ}, in terms of the coupling parameter λ.[12] The reduction in the computational cost with respect to AC is huge because the scaling goes down from M^6, where M is the number of the basis set functions, to only M^6_{active}, where M_{active} is the number of the active orbitals. Taking into account that AC0 requires neither construction of higher than second-order RDMs nor solving the full ERPA eigenequation (only diagonalization of small subblocks of $\mathcal{A}^{\lambda=0}$ is performed), the method allows for efficient treatment of large active spaces (not achievable for perturbation methods). One should notice that even though the exact AC integrand eq 2 deviates from linearity,[20] the AC0 approximation has already been proven to provide good accuracy for systems of singlet spin symmetry, cf. refs 11−13. To show the capabilities of both the AC and AC0 methods for other than singlet spin symmetries, we present results for two model systems, in which triplet states play a significant role—the oxygen and the nitrogen molecules. We also apply the AC0 method to singlet and triplet states of the challenging tetramethyleneethane (TME) diradical. The AC/AC0 performance is compared with the CASPT2 and the

DOI: 10.1021/acs.jpclett.9b01582
J. Phys. Chem. Lett. 2019, 10, 4668−4674

recently introduced multiconfiguration pair-density DFT (MC-PDFT) approach with the tPBE functional.[3,21] The latter, similarly to AC and AC0, requires only one- and two-electron reduced density functions to capture electron correlation, but because it employs density functionals, the computational cost is much lower than that of the other multireference methods and it is almost insensitive to the choice of basis set while AC and AC0 present a basis set dependence typical for ab initio methods (see comparison of the basis set dependency of CASSCF, AC, AC0, and tPBE results in the SI).

Diverse character of the excited states of the N_2 molecule provides a good test of accuracy for the AC and AC0 methods. For example, it is clear that the first triplet state, $^3\Sigma_u^+$, is already sufficiently described by the CAS(6,6) wave function (see Table 1). Notice, however, that AC, AC0, and MC-PDFT (specifically the employed tPBE functional[3]) enhance the accuracy even further, unlike CASPT2, which underestimates the excitation energy by 0.50 eV. For the remaining states, the inclusion of the dynamic correlation, provided by any of the tested approaches, improves their description. Both CASPT2 and tPBE tend to underestimate the excitations, while AC and AC0 slightly overestimate them. AC0 is clearly the most accurate in the group, outperforming even its more expensive relative, AC, which in turn performs better than both tPBE and CASPT2.

Table 1. Signed Errors and the Mean Unsigned Error (MAE) of the N_2 Adiabatic Singlet and Triplet Excitation Energies with Respect to the Experimental Values,[22,23] Given in eV[a]

	CAS	AC0	AC	tPBE	CASPT2
$^3\Sigma_u^+$	0.17	0.02	0.05	−0.11	−0.50
$^3\Pi_g$	2.01	0.08	0.48	−0.33	−0.38
$^3\Delta_u$	0.52	0.06	0.13	−0.22	−0.41
$^3\Sigma_u^-$	1.03	0.23	0.23	−0.09	−0.26
$^1\Pi_g$	2.38	0.27	0.63	−0.36	−0.24
$^1\Sigma_u^-$	0.82	0.07	0.15	−0.32	−0.35
$^1\Delta_u$	1.19	0.16	0.22	−0.73	−0.25
MAE	1.16	0.13	0.27	0.31	0.34

[a]All computations were performed for the CAS(6,6) reference in the aug-cc-pVTZ basis set.[24]

Both AC and AC0 are also capable of capturing the entire dissociation curves for triplet and singlet states of molecules, as evidenced for the O_2 molecule in Figure 1. Unlike tPBE, which predicts significantly deeper minima of both $^3\Sigma_g^+$ and $^1\Delta_g$ states, AC, AC0, and CASPT2 produce similar curves. Because the value of the S−T gap, 0.98 eV,[25] is already perfectly captured by the CASSCF approach (cf. Table 2), let us only mention that while AC0, AC, and CASPT2 maintain that accuracy (with −0.04, − 0.05, and −0.03 eV errors, respectively) tPBE performs slightly worse (with 0.20 eV of error). Because both AC0 and AC are size-consistent, to obtain the value of the bond dissociation energy (BDE) of the $^3\Sigma_g^+$ state, we employed the formula BDE = $E_{eq}(O_2) - 2E(O)$, where the energy E_{eq} corresponds to the equilibrium bond length, R_{OO} = 1.2 Å. The differences in accuracy of computed BDEs are more significant than those for the S−T gap. While CASSCF gives an error of −1.02 eV with respect to the experimental value,[26] each of the studied methods manages to improve on this value, with AC being the best performer (0.00 eV of error) followed by CASPT2 with −0.12 eV, AC0 (0.22 eV), and tPBE (0.77 eV).

In order to gain better insight into the performance of the AC and AC0 methods, in Figure 2 we present plots of the W_{AC} and

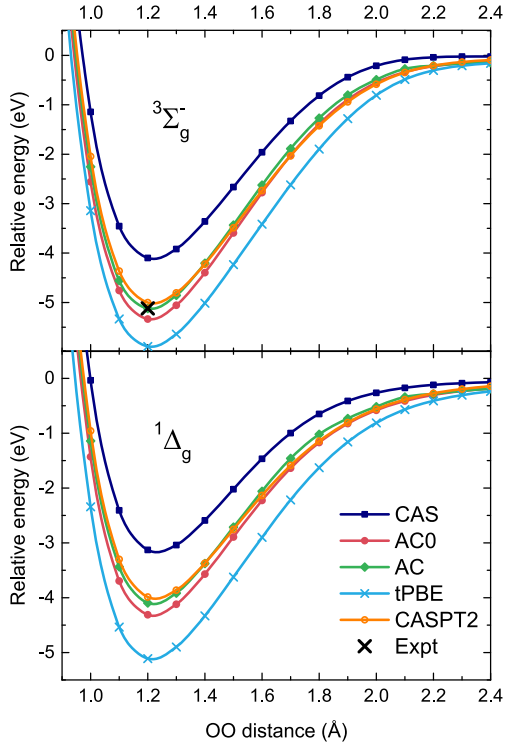

Figure 1. O_2 dissociation curves. All computations were performed with the cc-pVTZ basis set[24] using a CAS(12,8) reference. A cross in the upper panel indicates the experimentally obtained value of the dissociation energy.

Table 2. Signed Errors of the BDE of the $^3\Sigma_g^+$ State of O_2 and the S−T Gap at R_{OO} = 1.2 Å with Respect to the Experimental Values,[25,26] Given in eV[a]

	BDE	S−T
CAS	−1.02	0.01
AC0	0.22	−0.04
AC	0.00	−0.05
tPBE[b]	0.77	0.20
CASPT2	−0.12	−0.03
FCIQMC	−0.12	

[a]All computations were performed with the cc-pVTZ basis set[24] using (except for FCIQMC[27]) a CAS(12,8) reference. [b]Notice that in ref 28 the BDE values of O_2 computed with CASSCF (3.83 eV) and tPBE (5.59 eV, which is closer to the experimental value) differ from ours, probably due to the use of a single-state CASSCF by Odoh et al.

W_{AC0} integrands [cf. eq 11], yielding, respectively, AC or AC0 correlation energies. For the hydrogen molecule, we have also included plots of the exact integrands, W_{exact}, yielding exact correlation energies for a given singlet or triplet reference (the procedure for generating W_{exact} for two-electron singlet states has been presented in ref 20, while for triplets we have followed a similar procedure obtaining the transition density matrices for a given value of λ by solving the two-electron FCI equation with the AC Hamiltonian). The results in Figure 2 show that typically the AC0 curve is above the AC one; thus, AC0 recovers slightly less correlation than AC for both singlet and triplet states. This is because the W_{AC} integrands are typically slightly concave (one should notice that this is not the rule, and we have observed also cases when W_{AC} were convex). Another general observation is that, similarly to what has been already observed for singlet states, the curvature of the triplet AC integrands is small, which

DOI: 10.1021/acs.jpclett.9b01582
J. Phys. Chem. Lett. 2019, 10, 4668−4674

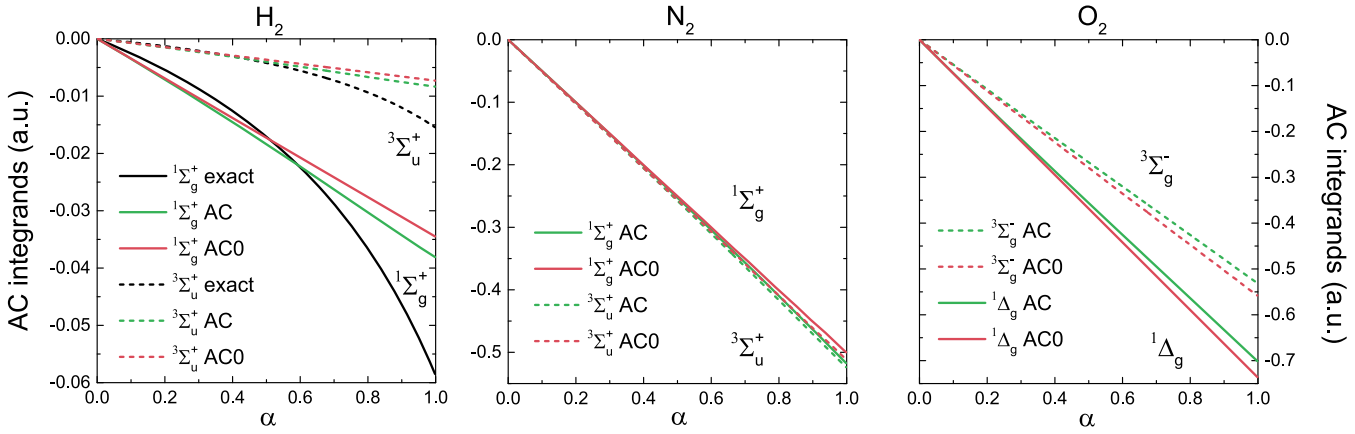

Figure 2. Exact AC integrands W_{exact}^{λ} for the lowest singlet and triplet state of H_2 and the AC and AC0 approximations, W_{AC}^{λ} and W_{AC0}^{λ}, of the lowest singlet and triplet states of H_2, N_2, and O_2. Computations were performed in the cc-pVTZ basis set for H_2 (R_{HH} = 1.401 au) and N_2 and in aug-cc-pVTZ for O_2 (geometries corresponding to the ones in Tables 1 and 2) and active spaces (2,2), (6,6), and (8,12) for H_2, N_2, and O_2, respectively.

provides justification for the AC0 approximation. The exact AC integrands obtained for the H_2 molecule are concave for both the singlet and triplet states. Evidently, integration of the nearly linear W_{AC} function yields correlation energies in errors of 2.2 mHa and 1.2 mHa for the singlet and triplet, and consequently, the S−T gap for H_2 is in error of only −0.03 eV with respect to the FCI value. For the N_2 and O_2 molecules, one can see that W_{AC0} follows rather closely the W_{AC} curves. Consequently, one expects that the accuracy of the singlet−triplet gaps from both methods will be comparable. In general, one cannot predict a priori which of the two methods will be superior. Notice, however, that AC0 results are obtained at the fraction of the cost of the AC method. In addition, the AC0 integrand is immune to potential instability problems in the ERPA equations that can deteriorate the accuracy of the AC method (cf., for example, the build-up of instability in the W_{AC} curve for the triplet Π_g state of the N_2 molecule, resulting in larger error of the AC excitation than that of the AC0 presented in Table 1).

Numerical evidence presented in this work shows that both AC and AC0 provide an excellent description of states of different spatial and spin symmetries. Moreover, it reinforces our previous observation[12,13] that the AC0 approach is comparable in accuracy with the much more computationally demanding AC method. It is therefore well justified to use this inexpensive method to capture the dynamic correlation in highly multireference states of larger systems.

Our final example is the TME molecule—a paradigm system for multireference methods trying to correctly balance both dynamic and static correlation.[29−35] The first challenge stems from disjoint biradical character of TME—two radical electrons localize on spatially separated parts of the molecule and the resulting frontier orbitals interact weakly and are nearly degenerate. The second challenge is due to the fact that the molecule may rotate about its central C−C bond and the multireference character of the singlet state is changing along this rotation. Correct description of the singlet surface together with correct ordering of both close-lying states at the entire range of the torsional potential turned out to be a perfect test for new multireference methods.[30,33] In their seminal work, Pozun et al.[30] applied diffusion Monte Carlo (DMC) and predicted the magnitude of the S−T gap to be as narrow as 0.02 eV for the angle of 45°. These findings were later corroborated by full configuration interaction quantum Monte Carlo (FCIQMC) calculations of Veis et al.[33] and are also in agreement with the available experimental data.[36]

The benchmark FCIQMC energy curve for the singlet state of TME, Figure 3, features a maximum at the torsional angle close to 45° and has two minima located at 0 and 90°, the former being slightly more stable. The lack of dynamic correlation in CASSCF with six π active orbitals leads to erroneous shape of

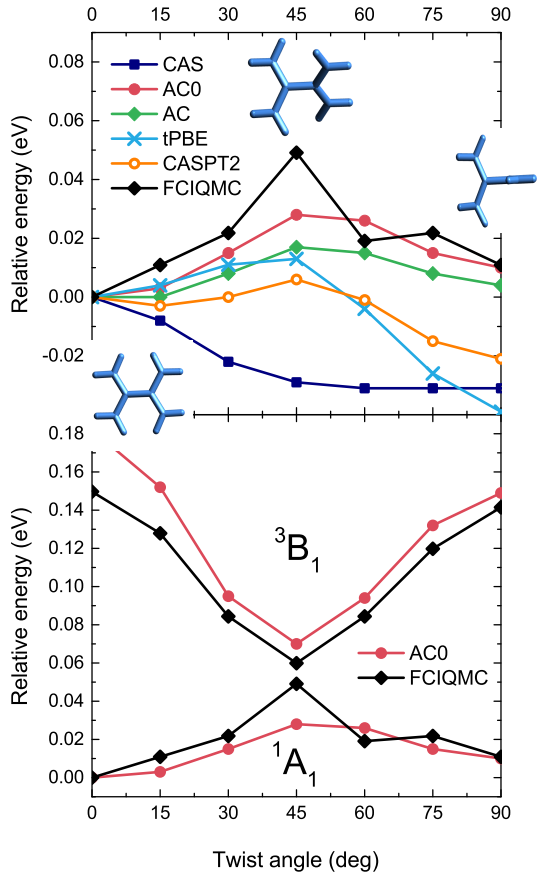

Figure 3. Singlet twisting curve of tetramethylethane (upper panel) and singlet and triplet twisting curves of tetramethylethane (lower panel). All computations were performed with the cc-pVTZ basis set[24] using (except for FCIQMC) a CAS(6,6) reference. The geometries used are the same as those in ref 33; they are provided in the SI.

DOI: 10.1021/acs.jpclett.9b01582
J. Phys. Chem. Lett. 2019, 10, 4668−4674

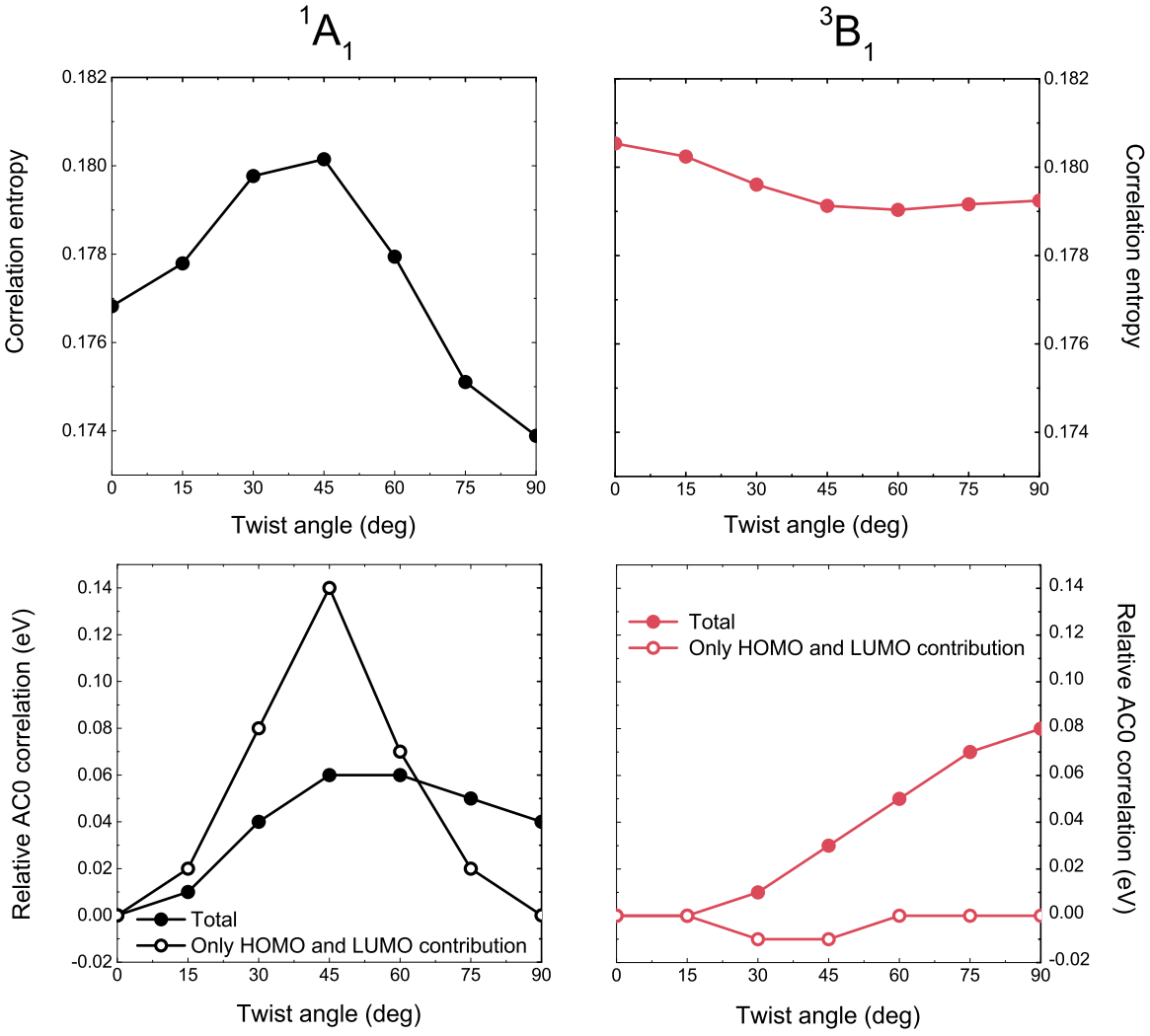

Figure 4. Correlation entropy (upper panel), relative AC0 correlation energy, and HOMO and LUMO contributions to the correlation energy (lower panel) for the singlet (left) and triplet (right) structures of TME.

the singlet potential. Notice that the correct shape is not recovered even if the active space is extended to 24 electrons in 25 orbitals.[33] Both CASPT2 and tPBE improve upon CASSCF and locate the maximum in the vicinity of 45°. One should note, however, that these methods significantly underestimate the twisting energy barrier with respect to the FCIQMC reference (see also Table S1 in the SI). Furthermore, neither CASPT2 nor tPBE succeeds at recognizing the $E(0°)$ minimum as the global one. This results from a too rapid decline in energy in the 45−90° range. As evidenced in Figure 3, AC approaches perform best out of the presented methods and correctly reproduce all of the main features of the singlet twisting potential. In particular, they are the only approaches that pinpoint the relative energies of the 0 and 90° minima. The triplet potential curve calculated at the AC0 level of theory (performance of the AC for triplet state parallels that of the AC0; see the SI) has the correct shape, and the resulting S−T gap reaches 0.04 eV in the most narrow point at 45°, which is only slightly overestimated with respect to the FCIQMC and DMC values (0.01 and 0.02 eV, respectively).

To gain a better insight into the interplay of dynamic and static correlation effects in the $^1A_1$ and $^3B_1$ states of TME, in Figure 4 we plot two quantities: the correlation entropy and the AC0 correlation energy. The former serves as a measure of the nondynamic correlation[37] and is defined as $S_{corr} = -\frac{1}{6}\sum_p n_p \ln n_p$ (the factor 1/6 comes from the fact that there are six active orbitals), while the latter corresponds to the dynamic correlation. Additionally, we plot contributions to the AC0 correlation energy originating solely from the HOMO and LUMO orbitals. Singling out contributions from a selected group of orbitals is feasible in AC0 by constraining the ERPA excitation operator. Upon twisting from 0 to 45°, one observes a steep rise of the correlation entropy for the $^1A_1$ state that indicates a pronounced multireference character. This effect is accompanied by a suppression of dynamic correlation (notice that lower panels in Figure 4 present relative correlation energy; thus, the pertinent curve goes up to larger values if the correlation energy decreases) with a substantial contribution from the frontier orbitals. Going from 45 to 90° results in a rapid drop in the static correlation diagnostic, S_{corr}. The concurrent increase in dynamic correlation is less pronounced, although the contribution from the HOMO and LUMO rises quickly. Thus, the cooperative effects of dynamic and nondynamic correlation involving frontier orbitals lead to a buildup of a maximum in the potential energy curve in a singlet state of TME. This resembles a typical covalent bond-breaking situation. The picture obtained for the triplet is qualitatively different. The correlation entropy

DOI: 10.1021/acs.jpclett.9b01582
J. Phys. Chem. Lett. 2019, 10, 4668−4674

declines only slightly in the 0−45° range and remains almost constant in the remaining part of the curve. The dynamic correlation decreases monotonically by a significant amount, which guarantees the correct shape of the potential, but the role of frontier orbitals in this process is practically irrelevant. Overall, the obtained picture confirms that the closely lying triplet is dominated by dynamic correlation, which can be effectively described by single-reference methods.[30]

In summary, we have derived the spin-free AC correlation formula for the correlation energy based on spin-preserving adaptation of the excitation operator. Both AC and AC0 approximations are now applicable to CASSCF reference functions in arbitrary spin states. The presented numerical results confirm excellent performance of the less computationally demanding AC0 approach, which agrees with our earlier observations for closed-shell systems.[12] Because the most expensive steps in AC0 scale as $M_{sec}^2M_{act}^4$, $M_{sec}M_{act}^5$ and M_{act}^6 (M_{sec} and M_{act} denoting the number of secondary and active orbitals, respectively), the method is applicable to large active spaces, where other ab initio approaches such as AC, CASPT2, or NEVPT2 might not be feasible. At the same time, for all systems studied in this work, AC0 performs in a more reliable manner than the density-functional-based MC-PDFT approach. We verified the performance of AC0 for the challenging case of the TME diradical. Our method reproduced the FCIQMC benchmark outperforming both CASPT2 and MC-PDFT and proved useful in obtaining additional insight into the interplay of dynamic and nondynamic correlation in the system.

■ ASSOCIATED CONTENT

Supporting Information

The Supporting Information is available free of charge on the ACS Publications website at DOI: 10.1021/acs.jpclett.9b01582.

Additional details of the computations, plots showing the basis set dependence of the dissociation energy values of the O_2 molecule, AC integrands for triplet states of the N_2 molecule, geometries of TME, and formulas for the spin-free ERPA matrices (PDF)

■ AUTHOR INFORMATION

Corresponding Authors

*E-mail: ewa.pastorczak@p.lodz.pl.
*E-mail: hapka@tiger.chem.uw.edu.pl.
*E-mail: pernalk@gmail.com.

ORCID

Ewa Pastorczak: 0000-0002-5046-1476
Michał Hapka: 0000-0001-7423-3198
Libor Veis: 0000-0002-4229-6335

Notes

The authors declare no competing financial interest.

■ ACKNOWLEDGMENTS

This work has been supported by the National Science Centre of Poland under Grant No. 2016/23/B/ST4/02848.

■ REFERENCES

(1) Toulouse, J.; Assaraf, R.; Umrigar, C. J. *Advances in Quantum Chemistry*; Elsevier, 2016; Vol. 73; pp 285−314.
(2) Fromager, E.; Toulouse, J.; Jensen, H. J. A. On the universality of the long-/short-range separation in multiconfigurational density-functional theory. *J. Chem. Phys.* **2007**, *126*, 074111.
(3) Li Manni, G.; Carlson, R. K.; Luo, S.; Ma, D.; Olsen, J.; Truhlar, D. G.; Gagliardi, L. Multiconfiguration Pair-Density Functional Theory. *J. Chem. Theory Comput.* **2014**, *10*, 3669−3680.
(4) Andersson, K.; Malmqvist, P. A.; Roos, B. O.; Sadlej, A. J.; Wolinski, K. Second-order perturbation theory with a CASSCF reference function. *J. Phys. Chem.* **1990**, *94*, 5483−5488.
(5) Andersson, K.; Malmqvist, P.-Å.; Roos, B. O. Second-order perturbation theory with a complete active space self-consistent field reference function. *J. Chem. Phys.* **1992**, *96*, 1218−1226.
(6) Angeli, C.; Cimiraglia, R.; Evangelisti, S.; Leininger, T.; Malrieu, J.-P. Introduction of n-electron valence states for multireference perturbation theory. *J. Chem. Phys.* **2001**, *114*, 10252−10264.
(7) Angeli, C.; Cimiraglia, R.; Malrieu, J.-P. *n*-electron valence state perturbation theory: A spinless formulation and an efficient implementation of the strongly contracted and of the partially contracted variants. *J. Chem. Phys.* **2002**, *117*, 9138.
(8) Andersson, K. Different forms of the zeroth-order Hamiltonian in second-order perturbation theory with a complete active space self-consistent field reference function. *Theor. Chim. Acta* **1995**, *91*, 31−46.
(9) Havenith, R. W.; Taylor, P. R.; Angeli, C.; Cimiraglia, R.; Ruud, K. Calibration of the n-electron valence state perturbation theory approach. *J. Chem. Phys.* **2004**, *120*, 4619−4625.
(10) Schapiro, I.; Sivalingam, K.; Neese, F. Assessment of n-electron valence state perturbation theory for vertical excitation energies. *J. Chem. Theory Comput.* **2013**, *9*, 3567−3580.
(11) Pernal, K. Electron Correlation from the Adiabatic Connection for Multireference Wave Functions. *Phys. Rev. Lett.* **2018**, *120*, 013001.
(12) Pastorczak, E.; Pernal, K. Correlation Energy from the Adiabatic Connection Formalism for Complete Active Space Wave Functions. *J. Chem. Theory Comput.* **2018**, *14*, 3493−3503.
(13) Pastorczak, E.; Pernal, K. Electronic Excited States from the Adiabatic-Connection Formalism with Complete Active Space Wave Functions. *J. Phys. Chem. Lett.* **2018**, *9*, 5534.
(14) McWeeny, R. The density matrix in many-electron quantum mechanics I. Generalized product functions. Factorization and physical interpretation of the density matrices. *Proc. Royal Soc. London, Ser. A* **1959**, *253*, 242−259.
(15) Rowe, D. J. Equations-of-Motion Method and the Extended Shell Model. *Rev. Mod. Phys.* **1968**, *40*, 153.
(16) Chatterjee, K.; Pernal, K. Excitation energies from extended random phase approximation employed with approximate one-and two-electron reduced density matrices. *J. Chem. Phys.* **2012**, *137*, 204109.
(17) Pernal, K.; Chatterjee, K.; Kowalski, P. H. How accurate is the strongly orthogonal geminal theory in predicting excitation energies? Comparison of the extended random phase approximation and the linear response theory approaches. *J. Chem. Phys.* **2014**, *140*, 014101.
(18) Oddershede, J.; Jørgensen, P.; Yeager, D. L. Polarization propagator methods in atomic and molecular calculations. *Comput. Phys. Rep.* **1984**, *2*, 33−92.
(19) Pernal, K. Intergeminal Correction to the Antisymmetrized Product of Strongly Orthogonal Geminals Derived from the Extended Random Phase Approximation. *J. Chem. Theory Comput.* **2014**, *10*, 4332−4341.
(20) Pernal, K. Exact and approximate adiabatic connection formulae for the correlation energy in multireference ground and excited states. *J. Chem. Phys.* **2018**, *149*, 204101.
(21) Stoneburner, S. J.; Truhlar, D. G.; Gagliardi, L. MC-PDFT can calculate singlet−triplet splittings of organic diradicals. *J. Chem. Phys.* **2018**, *148*, 064108.
(22) Larsen, H.; Olsen, J.; Jørgensen, P.; Christiansen, O. Full configuration interaction benchmarking of coupled-cluster models for the lowest singlet energy surfaces of N2. *J. Chem. Phys.* **2000**, *113*, 6677−6686.
(23) Larsen, H.; Hald, K.; Olsen, J.; Jørgensen, P. Triplet excitation energies in full configuration interaction and coupled-cluster theory. *J. Chem. Phys.* **2001**, *115*, 3015−3020.

DOI: 10.1021/acs.jpclett.9b01582
J. Phys. Chem. Lett. 2019, 10, 4668−4674

(24) Dunning, T. H., Jr. Gaussian basis sets for use in correlated molecular calculations. I. The atoms boron through neon and hydrogen. *J. Chem. Phys.* **1989**, *90*, 1007.
(25) Huber, K. P.; Herzberg, G. H. In *NIST Chemistry WebBook, NIST Standard Reference Database Number 69*; Linstrom, P., Mallard, W., Eds.; National Institute of Standards and Technology: Gaithersburg, MD, 2019; (data prepared by Jean W. Gallagher and Russell D. Johnson).
(26) Cosby, P. C.; Huestis, D. L. On the dissociation energy of O_2 and the energy of the O_2^+ $b^4\sum_g^-$ state. *J. Chem. Phys.* **1992**, *97*, 6108−6112.
(27) Kelly, T. P.; Perera, A.; Bartlett, R. J.; Greer, J. C. Monte Carlo configuration interaction with perturbation corrections for dissociation energies of first row diatomic molecules: C_2, N_2, O_2, CO, and NO. *J. Chem. Phys.* **2014**, *140*, 084114.
(28) Odoh, S. O.; Manni, G. L.; Carlson, R. K.; Truhlar, D. G.; Gagliardi, L. Separated-pair approximation and separated-pair pair-density functional theory. *Chem. Sci.* **2016**, *7*, 2399−2413.
(29) Borden, W. T.; Davidson, E. R. Effect of through-bond interaction on terminal methylene rotation in the tetramethylene diradical. *J. Am. Chem. Soc.* **1980**, *102*, 5409−5410.
(30) Pozun, Z. D.; Su, X.; Jordan, K. D. Establishing the Ground State of the Disjoint Diradical Tetramethyleneethane with Quantum Monte Carlo. *J. Am. Chem. Soc.* **2013**, *135*, 13862−13869.
(31) Brabec, J.; Banik, S.; Kowalski, K.; Pittner, J. Perturbative universal state-selective correction for state-specific multi-reference coupled cluster methods. *J. Chem. Phys.* **2016**, *145*, 164106.
(32) Chien, A. D.; Zimmerman, P. M. Recovering dynamic correlation in spin flip configuration interaction through a difference dedicated approach. *J. Chem. Phys.* **2017**, *146*, 014103.
(33) Veis, L.; Antalík, A.; Legeza, Ö.; Alavi, A.; Pittner, J. The Intricate Case of Tetramethyleneethane: A Full Configuration Interaction Quantum Monte Carlo Benchmark and Multireference Coupled Cluster Studies. *J. Chem. Theory Comput.* **2018**, *14*, 2439−2445.
(34) Lang, J.; Brabec, J.; Saitow, M.; Pittner, J.; Neese, F.; Demel, O. Perturbative triples correction to domain-based local pair natural orbital variants of Mukherjee's state specific coupled cluster method. *Phys. Chem. Chem. Phys.* **2019**, *21*, 5022−5038.
(35) Sinha Ray, S.; Manna, S.; Ghosh, A.; Chaudhuri, R. K.; Chattopadhyay, S. Multireference perturbation theory with improved virtual orbitals for radicals: More degeneracies, more problems. *Int. J. Quantum Chem.* **2019**, *119*, No. e25776.
(36) Clifford, E. P.; Wenthold, P. G.; Lineberger, W. C.; Ellison, G. B.; Wang, C. X.; Grabowski, J. J.; Vila, F.; Jordan, K. D. Properties of tetramethyleneethane (TME) as revealed by ion chemistry and ion photoelectron spectroscopy. *J. Chem. Soc., Perkin Trans. 2* **1998**, 1015−1022.
(37) Ziesche, P.; Smith, V. H., Jr; Hô, M.; Rudin, S. P.; Gersdorf, P.; Taut, M. The He isoelectronic series and the Hooke's law model: Correlation measures and modifications of Collins' conjecture. *J. Chem. Phys.* **1999**, *110*, 6135−6142.

DOI: 10.1021/acs.jpclett.9b01582
J. Phys. Chem. Lett. 2019, 10, 4668−4674